Astron. Astrophys. 337, 465–471 (1998)

ASTRONOMY AND ASTROPHYSICS

A near-infrared study of IRAS-selected T Tauri stars in Chamaeleon II

K.A. Larson[1,2], **D.C.B. Whittet**[1,⋆], **T. Prusti**[3], **and J.E. Chiar**[1,⋆,⋆⋆]

[1] Department of Physics, Applied Physics, & Astronomy, Rensselaer Polytechnic Institute, Troy, NY 12180, USA
[2] Anglo-Australian Observatory, Schmidt Telescope, Private Bag, Coonabarabran, NSW 2357, Australia
[3] ISO Science Operations Centre, Astrophysics Division, ESA, Villafranca del Castillo, P.O. Box 50727, E-28080 Madrid, Spain

Received 6 January 1998 / Accepted 10 June 1998

Abstract. We use near-infrared photometry of objects detected by IRAS to confirm four new T Tauri stars in Chamaeleon II. Observations of these sources generally agree with the T Tauri signatures of locus in the near-infrared color-color diagram, mid-infrared spectral index, and IRAS far-infrared colors. Infrared properties of these stars are similar to optically selected T Tauri stars in Cha II, but are on average more luminous and are located at the north-east boundary of star formation in the cloud. We compare results of infrared color methods used to detect T Tauri stars in Cha II with results of other methods based on optical and X-ray emission.

Key words: stars: pre-main-sequence – ISM: individual objects: Cha II – infrared: stars

1. Introduction

Understanding the processes of star formation continues to be one of the principal objectives of observational astronomy. In particular, infrared observations have been used to detect and study the earliest stages of star formation. Ground-based and space-based observations in wavebands ranging from $1\,\mu\mathrm{m}$ to beyond $100\,\mu\mathrm{m}$ detect emission from circumstellar dust surrounding young stellar objects (YSOs). Of the nearby Galactic star-forming regions, Chamaeleon II is especially well suited for infrared studies of star formation. With a compact clumpy structure and a distance of only 178 pc (Whittet et al. 1997), many faint pre-main-sequence (PMS) objects are observed with high spatial resolution over the one square degree extent of Cha II. Furthermore, at Galactic latitude $b \simeq -15°$, the line of sight is relatively simple with little foreground extinction (i.e. $E_{B-V} < 0.05\,\mathrm{mag}$ toward foreground stars, Whittet et al. 1997).

In the past decade, the YSO population and the star-formation mechanism, as well as the nature and evolution of the interstellar cloud material, have been investigated in the Chamaeleon complex. Many low-mass PMS objects, the T Tauri stars, have been observed in Cha II (e.g. Schwartz 1992, Gauvin & Strom 1992, Gregorio-Hetem et al. 1992, Alcalá et al. 1997). This paper searches for additional T Tauri stars in the ongoing effort to compile a complete census of YSOs in this cloud.

Near-infrared (NIR) photometry has already successfully confirmed the early evolutionary nature of many T Tauri stars in Cha II. Whittet et al. (1991) used NIR observations and measurements in the IRAS Serendipitous Survey and Point Source Catalogs to confirm the T Tauri status of ten Hα emission-line stars from the objective-prism catalog of Schwartz (1977). In addition, Whittet et al. (1991) observed the IRAS source 12496-7650 and confirmed that it is a very young, deeply embedded protostellar object (Hughes et al. 1989, 1991). In order to extend the optically-selected catalog of Whittet et al. (1991), Prusti et al. (1992) searched the IRAS Faint Source Catalog as well as the two catalogs listed above for additional sources in Cha II within the coordinates $12^{\mathrm{h}}44^{\mathrm{m}} < \mathrm{RA}(1950) < 13^{\mathrm{h}}10^{\mathrm{m}}$ and $-76°20' > \mathrm{Dec}(1950) > -77°45'$ and with detections in at least one waveband shorter than $100\,\mu\mathrm{m}$. Eight of the 30 sources in Prusti et al. (1992) have IRAS colors typical of YSOs.

The primary goal of this study is to confirm additional T Tauri stars in Cha II in order to extend the currently known inventory of star formation in the Chamaeleon region. A secondary goal is to compare the results of various techniques used to identify T Tauri stars. Agreement among various methods will lend further confidence in these methods. Alternatively, distinct populations detected with the various techniques can be contrasted and investigated for evidence of star-formation evolution. In Sect. 2 of this paper, we present NIR photometry for a subset of the objects identified in Prusti et al. (1992). Analyses of these data to identify and characterize PMS objects are described in Sect. 3, and will closely follow the methods of Whittet et al. (1991). Results of these analyses are discussed in Sect. 4. This paper will conclude with a comparison of infrared excess to other spectral signatures used to confirm T Tauri status.

Send offprint requests to: K. Larson

⋆ Visiting astronomer, Cerro Tololo Inter-American Observatory, National Optical Astronomy Observatories, which are operated by the Association of Universities for Research in Astronomy, under contract with the National Science Foundation

⋆⋆ Present address: NASA Ames Research Center, Mail Stop 245–3, Moffett Field, CA 94035, USA

Correspondence to: Department of Physics, Applied Physics, & Astronomy, Rensselaer Polytechnic Institute, Troy, NY 12180, USA (kal@charon.phys.rpi.edu)

Table 1. Near-infrared positions and photometry

#	IRAS name	RA(1950)	Dec(1950)	J	H	K	L
1	12448-7650	12:44:53.4	−76:50:17	6.87	5.61	5.19	4.89
2	F12451-7632[a]	12:45:08.9	−76:32:43	8.50	7.00	6.49	6.18
4	F12471-7643[a]	12:47:07.6	−76:44:02	8.47	7.21	6.83	6.58
6	F12486-7744[a]	12:48:36.1	−77:44:10	8.63	7.48	7.16	6.91
7	F12488-7658[a]	12:48:52.7	−76:58:47	9.22	7.82	7.34	6.90
10	F12520-7631	12:52:01.1	−76:31:27	7.94	6.70	6.36	6.01
13	12535-7623	12:53:30.7	−76:23:48	9.97	8.74	8.24	7.57
16	F12555-7638	12:55:31.1	−76:38:35	7.26	6.17	5.90	5.66
17	12556-7731	12:55:37.2	−77:30:52	8.08	6.92	6.62	6.43
20	12580-7716	12:58:05.0	−77:16:58	4.78	3.60	3.28	3.01
21	F12584-7702	12:58:22.5	−77:02:04	8.63	7.12	6.61	6.29
22	12584-7621	12:58:26.4	−76:21:46	10.10	9.11	8.45	7.46
24	12589-7646	12:58:57.8	−76:46:35	7.42	6.25	5.87	5.53
25	13003-7735	13:00:20.1	−77:34:53	6.65	5.45	5.09	4.84
26	13005-7633	13:00:33.4[c]	−76:34:01[c]	9.65	8.77	8.38	7.66
28	F13038-7649[a]	13:03:51.4	−76:49:51	8.19	7.12	6.86	6.65
29	F13049-7701[a]	13:04:50.8	−77:01:45	7.58	6.79	6.63	6.44
30	F13052-7653[a]	13:05:12.0[d]	−76:53:52[d]	10.09	9.22	8.84	8.32[b]

[a] IRAS Faint Source Reject Catalog, version 2.0
[b] $\sigma = 0.06$
[c] Two stars, 3″ separation. Both components included in aperture; mean position given.
[d] Three stars, 4″ separation. All components included in aperture; mean position given.

2. Near-infrared observations

Program stars were chosen from the list of 30 Cha II IRAS sources in Prusti et al. (1992). Only candidates with 12 μm detections and probable optical counterparts visible on the ESO/SRC photographic plates were selected. Embedded protostellar objects at too early an evolutionary stage to be detected in NIR and mid-infrared passbands may be among the excluded objects: indeed, four of the excluded objects have IRAS colors characteristic of embedded protostars. Of the 18 selected objects, IRAS colors suggest that six are T Tauri candidates and four are normal stars; the remaining eight have upper limits in all IRAS bands except 12 μm (Prusti et al. 1992). NIR observations of the selected sources were first attempted with the 1.5 m telescope of the Cerro Tololo Interamerican Observatory (CTIO) in Chile during 1992 May and 1993 June. The instrument used was a 58×62 pixel InSb array. NIR counterparts of the IRAS sources were identified at 2.2 μm, and positional measurements obtained, during non-photometric conditions on 1993 June 5, but no photometric measurements proved possible at CTIO. Photometric observations of the 18 program stars were obtained subsequently at the South African Astronomical Observatory (SAAO) in 1995 April 12–17. The Mark III InSb single-channel Infrared Photometer was used on the 1.9 m telescope to give magnitudes in standard J (1.25 μm), H (1.65 μm), K (2.2 μm), and L (3.5 μm) passbands. An 18″ aperture was used with a 30″ north-south chop. Results were reduced to the standard photometric system of Carter (1990). Data from multiple nights were averaged, with each measurement weighted by its formal statistical error.

In Table 1, positions of counterparts to the IRAS sources at 2.2 μm are listed in columns 3–4. Results are from the 1.5 m CTIO telescope pointing and are believed accurate to $\pm 3''$. Photometric magnitudes measured at SAAO in the *JHKL* passbands are listed in columns 5–8.

The photometric aperture includes all components of visual multiple stars (objects #26 and #30). Unless otherwise noted, the uncertainty in the *JHKL* magnitudes is equal to or less than standard values of $\sigma_J = 0.02$, $\sigma_H = 0.02$, $\sigma_K = 0.03$, and $\sigma_L = 0.05$. Column 1 of Table 1 lists the identification number assigned by Prusti et al. (1992) to identify sources in accompanying figures. Column 2 maintains the naming convention of Prusti et al. (1992), in which source names preceded by the letter F were found solely in the Faint Source Catalog. However, it should be noted that some of these sources have since been rejected from version 2.0 of the Faint Source Catalog. Data for some sources at the right ascension edges of the Cha II complex (see footnote for Table 1) are in the Faint Source Reject Catalog possibly because these areas of the sky were covered by fewer than six detector passes in pointed observations. In subsequent papers, the source names of Faint Source Reject Catalog members should be preceded by the letter Z.

3. Analyses

3.1. Infrared spectral index

An indication of PMS status can be obtained by calculating the mid-infrared spectral index, a, defined as the slope of the spectral energy distribution (SED) plotted $\log(\lambda F_\lambda)$ as a function of $\log \lambda$ from 2.2 μm to 25 μm (Wilking 1989). Sources with $a > 0$ and broad SEDs are categorized as class I. Infrared emission from these deeply embedded protostars still in the accretion phase is dominated by thermal radiation from cool dust. Class

Table 2. Spectral index, class, and extinction

#	IRAS name	a	Class	A_V
1	12448-7650	-2.14	III	3
2	F12451-7632	-2.46	III	5
4	F12471-7643	-2.41	III	3
6	F12486-7744	-2.22	III	2
7	F12488-7658	-2.09	III	4
10	F12520-7631	-2.46	III	3
13	12535-7623	-0.76	II	5
16	F12555-7638	-2.26	III	2
17	12556-7731	-1.61	(II)	2
20	12580-7716	-2.76	III	2
21	F12584-7702	-2.31	III	5
22	12584-7621	-0.68	II	1
24	12589-7646	-2.05	III	2
25	13003-7735	-2.56	III	3
26	13005-7633	-0.83	II	2
28	F13038-7649	-2.45	III	2
29	F13049-7701	-2.52	III	0
30	F13052-7653	-1.04	II	2

II sources are characterized by less infrared excess and spectral index $0 > a > -2$. These objects are usually T Tauri PMS stars with emission both from the stellar photosphere and from circumstellar dust at a range of temperatures. Class III stars, with spectral index $a < -2$, are indistinguishable from field stars based on spectral index alone. An unreddened blackbody in the Rayleigh-Jeans limit has spectral index $a = -3$.

To calculate the spectral index, the IRAS data from Prusti et al. (1992) are first color corrected (see IRAS Explanatory Supplement 1988). In cases with upper limits at 60 μm, a correction determined from the shorter passbands is applied. In cases with upper limits at 25 μm, the data are left uncorrected. In every case, the correction applied to the flux is less than 38%. This corresponds to a correction of about 7% in the logarithmic SED from 2.2 μm to 25 μm, and does not alter spectral classification in any case. We calculate spectral index as the slope of a line fit to the K, L, 12 μm, and 25 μm points using unweighted least-squares minimization. In cases where the flux at 25 μm is an upper limit, a line is fit to the K, L, and 12 μm points only. The spectral index and corresponding classification for each object is listed in columns 3 and 4 of Table 2.

A histogram of spectral index values for program stars is displayed in Fig. 1 as the solid line. For comparison, a histogram of the Cha II PMS emission-line stars from Whittet et al. (1991) is superimposed as the broken line. For clarity, we do not include previously identified field stars in the figures of this paper. The five sources in this study with $a > -2$ are labeled: 12535-7623 (#13), 12556-7731 (#17), 12584-7621 (#22), 13005-7633 (#26), and F13052-7653 (#30). It should be noted that 12556-7731 (#17) has a spectral index only marginally distinct from that of the field stars.

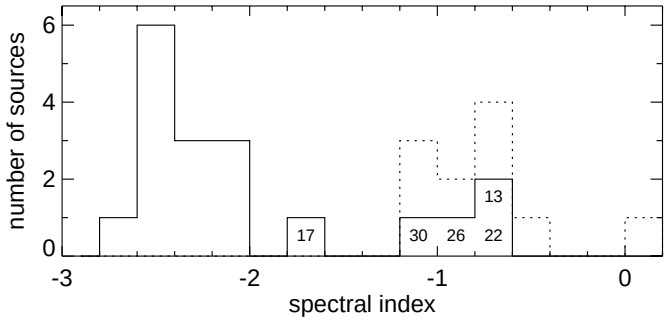

Fig. 1. Histogram of spectral index for program stars (Table 2, solid squares) and T Tauri stars from Whittet et al. (1991, broken line). Source numbers are from column 1 of Tables 1–3.

3.2. Near-infrared color-color diagram

Fig. 2 plots the $J - H$, $H - K$ color-color diagram for program stars (solid squares) as well as previously identified PMS emission-line stars in Cha II (Whittet et al. 1991, open squares). The five class II objects in our program are labeled. The loci of points occupied by unreddened dwarf and giant stars are shown as solid and dashed lines, respectively (Bessell & Brett 1988). Also shown is the reddening vector for interstellar extinction,

$$\frac{E_{J-H}}{E_{H-K}} = 1.61$$

(Whittet 1988). Stars that can be de-reddened along lines with this slope onto intrinsic color curves for giants probably are reddened giant field stars lying beyond the cloud. The dotted line in Fig. 2 is the locus of unreddened classical T Tauri stars as measured in the Taurus dark cloud and confirmed in accretion disk models by Meyer et al. (1997). Note that most of the previously identified PMS stars (open squares in Fig. 2) can be easily dereddened onto the dotted line.

Extinction maps of Cha II derived from stellar number density variation show clumpy structure with some regions of $A_V > 3$ mag (Gregorio-Hetem et al. 1988). Furthermore, the fact that the 100 μm emission is generally correlated with estimates of extinction in Cha II suggests that $A_V < 5$ mag (Prusti et al. 1992). If we rewrite the R_V-independent infrared extinction law (Martin & Whittet 1990) as $E_{J-H} \sim 0.13 A_V$, we can estimate foreground visual extinction from the color-color diagram. By the vertical extent to which presumed field stars and T Tauri stars are displaced along the reddening vector from their respective intrinsic color curves in Fig. 2, we deduce that the foreground visual extinction toward these objects ranges from zero to five magnitudes, consistent with other measurements of the Cha II cloud environment. Estimates of cloud extinction, accurate to about ± 1 mag, are listed in column 5 of Table 2.

3.3. Luminosity of T Tauri candidates

The SEDs of the five class II objects in our program are shown in Fig. 3. The error bars on the NIR points are smaller than the size of the plotting symbols. Downward-pointing arrows indicate that the IRAS points are upper limits. An estimate of

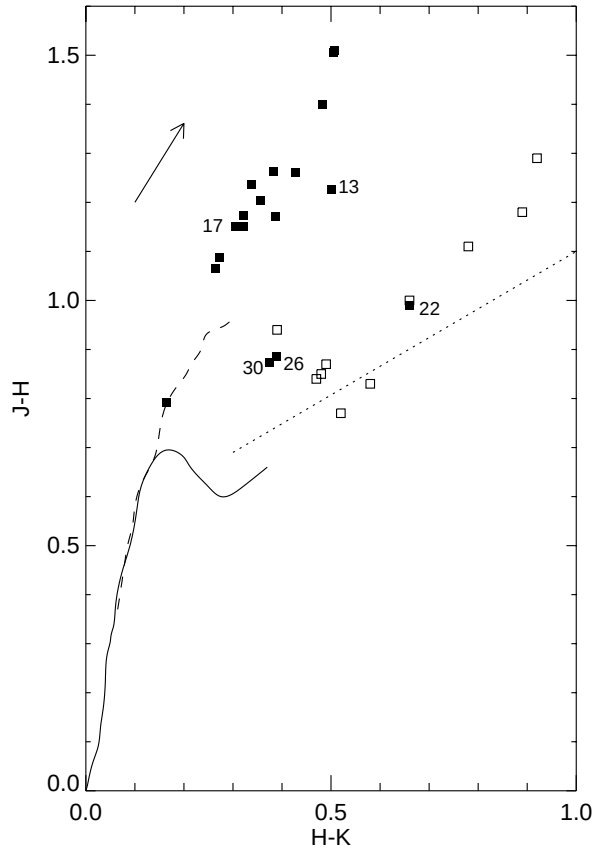

Fig. 2. Near-infrared color-color diagram for program stars (Table 1, solid squares) and T Tauri stars from Whittet et al. (1991, open squares). Source numbers are from column 1 of Tables 1–3. Intrinsic color curves for giant and dwarf luminosity classes are shown as dashed and solid lines, respectively (Bessell & Brett 1988). Vector represents direction of interstellar reddening (Whittet 1988). Dotted line represents intrinsic locus of classical T Tauri stars (Meyer et al. 1997).

the luminosity of each source can be obtained by integrating flux over wavelength,

$$L_{bol} = 4\pi d^2 \int_0^\infty F_\lambda d\lambda.$$

The distance, d, to Cha II was recently determined to be 178 ± 18 pc (Whittet et al. 1997). Straightforward trapezoidal integration under the NIR and IRAS photometry gives the observed luminosity, L_{obs}, of each embedded object. To extrapolate each SED to shorter wavelengths, a blackbody is fit to the NIR photometry and integrated shortward of J. Note that all five distributions in Fig. 3 peak near H. To estimate each SED at longer wavelengths, the IRAS detections are linearly extrapolated out to 100 μm. The short and long wavelength corrections are then added to L_{obs} yielding L_{bol}, which is listed in Table 3 for the class II objects. In this approximation, luminosity lost due to cloud extinction as well as significant luminosity beyond observed passbands are ignored. Thus, the calculated luminosity in Table 3 is still only a lower limit on the true luminosity of each source. The luminosity of the remaining class II object, 12556-7731 (#17), will be discussed in Sect. 4.

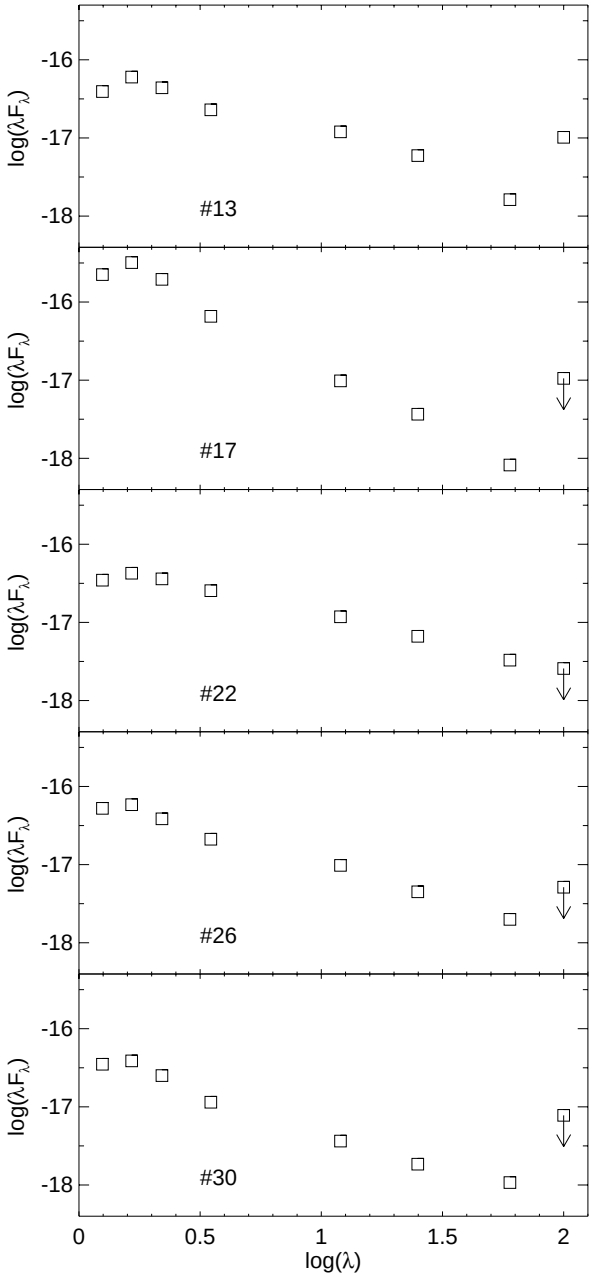

Fig. 3. Spectral energy distributions of candidate T Tauri stars. Units of λF_λ and λ are W cm^{-2} and μm, respectively. Source numbers are from column 1 of Tables 1–3. Arrows indicate upper limits.

4. Discussion

4.1. Identifying T Tauri stars

We can compare results of the three analytical tools described above to identify the T Tauri stars in our program. In the color-color diagram (Fig. 2), embedded T Tauri stars lie below the reddened field stars, but are located above the locus of intrinsic T Tauri colors (dotted line in Fig. 2) due to foreground extinction. Object 12584-7621 (#22) is clearly displaced below the field stars and does not lie along the reddening vector from the dwarf or giant intrinsic color curves. Objects 13005-7633 (#26)

Table 3. Luminosity of T Tauri stars

#	IRAS name	$L_{bol}/L_{\odot}$
13	12535-7623	1.33
22	12584-7621	1.27
26	13005-7633	1.32
30	F13052-7653	0.73

and F13052-7653 (#30) are also displaced below the field stars and have similar colors to T Tauri stars in Whittet et al. (1991, open squares in Fig. 2). Although they appear to lie along the interstellar reddening vector from the colors of K and M dwarfs, they are too bright to be late-type stars located beyond and reddened by the Cha II cloud. Because the luminosity of K and M dwarfs is less than $0.4\,L_{\odot}$ (Allen 1973), if any of the class II objects in our program were late-type dwarfs, they could not be located behind Cha II but instead would have to be at a much smaller distance, in front of Cha II, and thus unreddened. We therefore conclude that they must be YSOs embedded in the Cha II cloud.

The distinction between T Tauri stars and field stars can be most clearly seen in the histogram (Fig. 1). The three candidates (#22, #26, #30) suspected to be T Tauri stars from the NIR color-color diagram (Fig. 2) also have spectral index $a > -2$, clearly displaced from the group of normal field stars. The object 12535-7623 (#13) has a similarly high infrared excess and thus high spectral index. In the color-color diagram, this source is displaced slightly below the field stars. However, if de-reddened by $A_V \sim 2$–3 mag of interstellar extinction, 12535-7623 (#13) would then lie very near the other T Tauri stars in the color-color diagram. Foreground extinction listed in Table 2 for this object is based on its distance from the locus of unreddened T Tauri stars in Fig. 2.

The last class II object, 12556-7731 (#17), has a spectral index only marginally distinguished from that of the field stars in class III. In addition, the position of this source in the color-color diagram (Fig. 2) is well within the locus of points for normal field stars. Thus, the evidence of PMS status for this object is not conclusive based on both infrared color and spectral index. As can be seen in Fig. 3, the qualitative shape of the 12556-7731 (#17) curve, peak at H and slight excess at $12\,\mu$m and $25\,\mu$m relative to the continuum suggested by K and L, are similar to that of the unambiguous T Tauri stars 12535-7623 (#13) and 13005-7633 (#26). However, as compared to the other sources in Fig. 3, this object has much more NIR flux, while still relatively little far-infrared flux, i.e. less infrared excess.

If we do assume that 12556-7731 (#17) is embedded in Cha II and is thus at a distance of 178 pc, estimating the luminosity as described in Sect. 3.3 yields $4.10\,L_{\odot}$. Therefore, if embedded in the Cha II cloud, this object would be much more luminous than the unambiguous T Tauri stars in our program. In fact, Whittet et al. (1991) observed a complete lack of class II T Tauri stars in Cha II with luminosity $> 2\,L_{\odot}$. In general, it is the younger deeply-embedded class I objects that have relatively high infrared luminosity. However, it is extremely unlikely that 12556-7731 (#17) is one of these young class I objects; its SED does not rise, but instead steeply decreases through the mid-infrared passbands. It is possible that the luminosity of the object varied in the intervening years between the IRAS observations and our NIR observations. Also, the optical source may not correspond to the IRAS source; the NIR position is 4.″6 from the IRAS position. However, since the size of the IRAS uncertainty ellipse in that direction is 2.″5 and the NIR position has an uncertainty of 3″, it is reasonable that the optical source is indeed 12556-7731 (#17).

Therefore, we deduce that 12556-7731 (#17) is a reddened M giant by its position in the color-color diagram (Fig. 2). Applying a universal infrared extinction law (Martin & Whittet 1990) and a spectral type of M0 III, dereddening the K magnitude implies that the star is over 1 kpc away. It is unlikely that 12556-7731 (#17) is associated with the Cha II cloud at all. Like 13022-7650, another Cha II field star with a marginally class II SED, this object may be a distant field star with intrinsic $12\,\mu$m and $25\,\mu$m emission due to grain formation in the cool stellar photosphere (Whittet et al. 1991).

Finally, to conclusively identify T Tauri stars in this program from analyses of infrared photometry, it is necessary to include evidence from the IRAS color-color diagram (Prusti et al. 1992, reproduced in Fig. 4). All of the class II objects in our program have [60/25] and [25/12] colors characteristic of T Tauri stars. One additional object in our program, F12555-7638 (#16), has marginally characteristic T Tauri IRAS colors, but shows no NIR evidence of being a YSO and probably is a field star. Based on the agreement among the NIR color-color diagram (Fig. 2), mid-infrared spectral index (Fig. 1), and IRAS color-color diagram (Fig. 4), we conclude that 12535-7623 (#13), 12584-7621 (#22), 13005-7633 (#26), and F13052-7653 (#30) unambiguously are T Tauri stars. These results support findings of Gregorio-Hetem et al. (1992) in which #22 and #13 were shown to have both IRAS colors and optical spectra typical of T Tauri stars.

4.2. Comparison with other detection methods

Given the general agreement among the infrared color and spectral index analyses presented in this paper, it is useful to compare this technique with other observational methods used to find T Tauri stars. For example, detection of Hα emission lines generated at the interface between stellar photospheres and circumstellar accretion disks has been an effective tool in the discovery of YSOs. Whittet et al. (1991) showed that the Cha II Hα emission stars of Schwartz (1977) also exhibit the infrared signatures of T Tauri stars. A new objective prism survey of Cha II by Hartigan (1993) found four new Hα stars, including 13005-7633 (#26). The only other T Tauri star in this program within the Hartigan (1993) survey area, F13052-7653 (#30), was not detected as an Hα emission star. As compared to the emission-line PMS stars of Whittet et al. (1991), the average infrared luminosity of the T Tauri stars in the current paper is somewhat higher.

Without spectral type information, the distribution of these objects in the Hertzsprung-Russell diagram is not known. How-

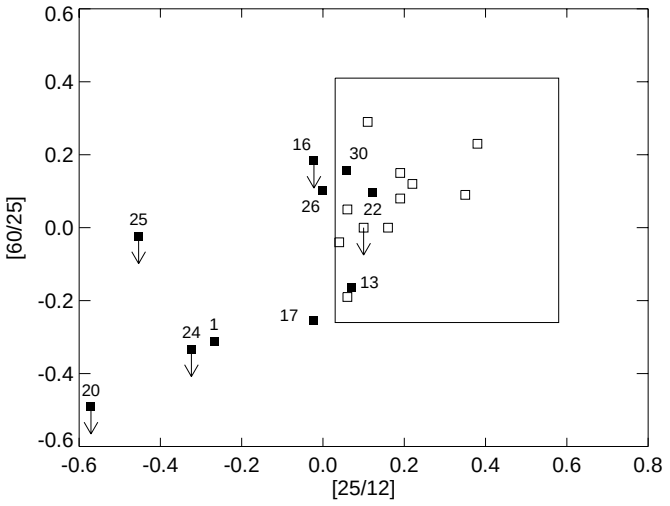

Fig. 4. IRAS color-color diagram for program stars (solid squares), reproduced from Prusti et al. (1992). Source numbers are from column 1 of Tables 1–3. T Tauri stars from Whittet et al. (1991, open squares) are shown for comparison. Sources with only upper limits are indicated with arrows pointing toward true location. Inner box shows definition T Tauri IRAS colors (Harris et al. 1988).

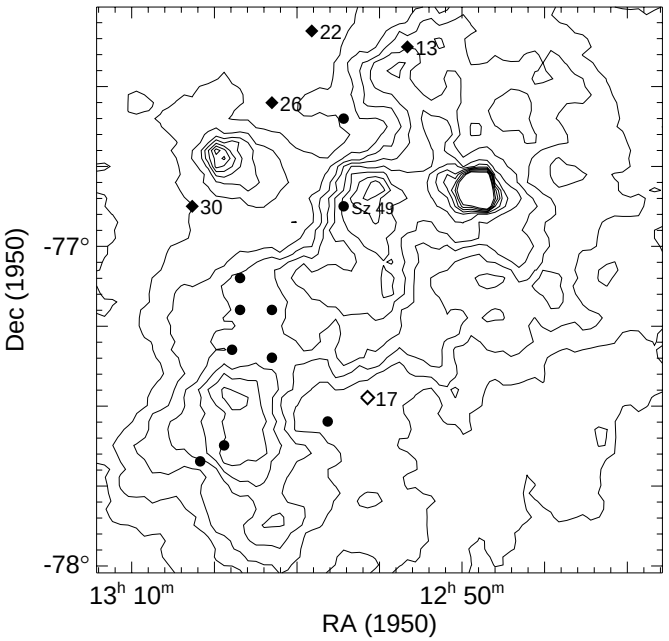

Fig. 5. Positions of new T Tauri stars (solid diamonds) and optically-identified T Tauri stars (Whittet et al. 1991, solid circles) relative to $100\,\mu\mathrm{m}$ emission in Cha II. Intensity contours shown from 2.5 to $40\,\mathrm{MJy\,sr^{-1}}$ in steps of $2.5\,\mathrm{MJy\,sr^{-1}}$. Source numbers are from column 1 of Tables 1–3. Source #17 (open diamond) has conflicting infrared T Tauri signatures; see text for discussion.

ever, the higher average luminosity of stars in this program may possibly imply that they are younger than those detected in the objective prism survey of Schwartz (1977). T Tauri stars which are detected in the infrared but not in optical emission lines may be more deeply embedded and at an earlier stage of evolution, during which dust both obscures the star and emits thermal radiation in the infrared. On the other hand, the spectral index distribution of sources in this study is similar to that of the optical emission-line stars studied by Whittet et al. (1991) as shown in Fig. 1.

Another complementary method used to find PMS stars is the search for X-ray emission. T Tauri stars without dense circumstellar material ("naked" T Tauri stars) will not show infrared excess; stars completely obscured by dust will not be detected in Hα emission. Instead, so-called weak-lined T Tauri stars have been found via their coronal X-ray emission. Using the ROSAT All-Sky Survey (RASS), Alcalá et al. (1995) found 77 T Tauri candidates in the Chamaeleon complex, 50% of which were confirmed with high-resolution spectroscopy by Covino et al. (1997). Of these confirmed objects, one is within the coordinate box of this study. This object corresponds to the Hα emission source Sz 49 (Schwartz 1977). The infrared color, spectral index, and SED of this object (Whittet et al. 1991) are indistinguishable from the other classical T Tauri stars in our program. This is somewhat surprising, as classical T Tauri stars are not typically X-ray luminous enough to be detected with RASS (Neuhäuser 1997).

In contrast to other classical T Tauri stars in the cloud, the new T Tauri stars in our study are not localized to the Cha II clumps. In Fig. 5, the positions of the new T Tauri stars (diamonds) and optically-selected T Tauri stars (Whittet et al. 1991, circles) are shown relative to the IRAS $100\,\mu\mathrm{m}$ emission. The new T Tauri stars with lowest foreground extinction, 12584-7621 (#22), 13005-7633 (#26), and F13052-7653 (#30), are located beyond the $I(100\,\mu\mathrm{m}) \sim 2.5\,\mathrm{MJy\,sr^{-1}}$ boundary of the cloud. Relative to the Hα emission-line stars, including the object also detected in X-ray emission (Alcalá et al. 1995, "Sz 49" in Fig. 5), the new T Tauri stars in this study are at the north-east edge of star-formation in the cloud, just beyond a steep density gradient. In order to evaluate the relative spatial distribution of YSO populations detected via infrared excess, Hα, and X-ray emission, the survey for infrared excess must be extended to cover many square degrees, comparable to the area covered by X-ray and Hα surveys.

Finally, new ISO data have extended infrared photometric studies of star formation into the $6.75\,\mu\mathrm{m}$ and $15\,\mu\mathrm{m}$ bands with a sensitivity about 50 times better than IRAS, permitting studies of the lowest-luminosity YSOs. Nordh et al. (1996) showed that YSOs in Chamaeleon have a higher relative [15]–[6.75] color than normal field stars, finding at least three YSOs in a limited-area survey of Cha II. Comparison of these objects with those found in IRAS studies will further define the stellar properties and relative spatial distribution of this sample. In addition, detailed modeling of the photometric and spectroscopic data will clarify which population is detected with infrared excess, relative to the populations detected in X-ray or optical line emission.

5. Conclusion

We have obtained near-infrared photometry of selected sources in an unbiased list of all IRAS Faint Source Catalog and Serendipitous Survey Catalog objects in Cha II. From analyses of the infrared colors and spectral energy distributions of these objects, we identify four T Tauri stars: 12535-7623 (#13), 12584-7621 (#22), 13005-7633 (#26), and F13052-7653 (#30). Three of these stars form the north-east edge of star formation in the Cha II cloud and are located beyond the steep density gradient and 100 μm emission boundary. These T Tauri stars are similar in their infrared properties to the Hα emission stars studied by Whittet et al. (1991), but are on average more luminous with $L_{bol} \sim 0.7$–$1.3\,L_{\odot}$ and thus may be slightly younger. An unbiased deep infrared survey over a wider area around the Chamaeleon complex will help clarify the correlation between properties of young stellar populations and the local cloud environment.

Acknowledgements. We are grateful to the Director of the South African Astronomical Observatory for the award of time on the 1.9 m telescope at SAAO. This research is partially funded by Rensselaer Polytechnic Institute, the Small Research Grants Program of the American Astronomical Society, and the NASA Specialized Center of Research and Training in Origins of Life. It has made use of the SIMBAD database, operated by the Centre des Données Stellaires in Strasbourg, and the SkyView on-line facility, operated by the HEASARC at NASA Goddard Space Flight Center. K.A.L. and J.E.C. acknowledge receipt of fellowships from the U.S. Department of Education. J.E.C. currently holds a National Research Council–ARC Research Associateship. K.A.L. thanks the Astronomer-in-Charge and staff at the Anglo-Australian Observatory Schmidt Telescope for their generous hospitality during the preparation of this paper.

References

Allen, C.W., 1973, Astrophysical Quantities, Athlone Press
Alcalá, J.M., Krautter, J., Schmitt, J.H.M.M., Covino, E., Wichmann, R., & Mundt, R. 1995, A&AS, 114, 109
Alcalá, J.M., Krautter, J., Covino, E., Neuhäuser, R., Schmitt, J.H.M.M., & Wichmann, R. 1997, A&A, 319,184
Bessell, M.S., & Brett, J.M. 1988, PASP, 100, 1134
Carter, B.S. 1990, MNRAS, 242, 1
Covino, E., Alcalá, J.H., Allain, S., Bouvier, J., Terranegra, L., & Krautter, J. 1997 A&A, 328, 187
Gauvin, L.S., & Strom, K.M. 1992, ApJ, 385, 217
Gregorio-Hetem, J.C., Sanzovo, G.C., & Lépine, J.R.D. 1988, A&AS, 76, 347
Gregorio-Hetem, J., Lépine, J.R.D., Quast, G.R., Torres, C.A.O., & de la Reza, R. 1992, AJ, 103, 549
Harris, S., Clegg, P., & Hughes, J. 1988, MNRAS, 235, 441
Hartigan, P. 1993, AJ, 105, 1511
Hughes, J.D., Emerson, J.P., Zinnecker, H., & Whitelock, P.A. 1989, MNRAS, 236, 117
Hughes, J.D., Hartigan, P., Graham, J.A., Emerson, J.P., & Marang, F. 1991, AJ, 101, 1013
IRAS Catalogs and Atlases: Explanatory Supplement 1988, C.A. Beichman, G. Neugebauer, H.J. Habing, P.E. Clegg & T.J. Chester (eds.), GPO, Washington
Martin, P. G., & Whittet, D. C. B. 1990, ApJ, 357, 113
Meyer, M. R., Calvet, N., & Hillenbrand, L. A. 1997, AJ, 114, 288
Neuhäuser, R. 1997, Science, 276, 1363
Nordh, L., Olofsson, G., et al. 1996, A&A, 315, L185
Prusti, T., Whittet, D.C.B., Assendorp, R., & Wesselius, P.R. 1992, A&A, 260, 151
Schwartz, R.D. 1977, ApJS, 35, 161
Schwartz, R.D. 1992, in Low Mass Star Formation in Southern Molecular Clouds, B. Reipurth (ed.), ESO Scientific Report No. 11, 93
Whittet, D.C.B. 1988, in Dust in the Universe, M.E. Bailey, & D.A. Williams (eds.), Cambridge University Press, 25
Whittet, D.C.B., Assendorp, R., Prusti. T., Roth, M., & Wesselius, P.R. 1991, A&A, 251, 524
Whittet, D.C.B., Prusti, T., Franco, G.A.P., Gerakines, P.A., Kilkenny, D., Larson, K.A., & Wesselius, P.R. 1997, A&A, 327, 1194
Wilking, B.A. 1989, PASP, 101, 229